Thin-Film Photovoltaics Partnership Program

First Quarterly Status Report – Year III

Covering the period of October 2, 2003 to January 1, 2004

Deliverable: Subcontract Article 3 B, **Item 14 (**ADJ-2-30630-13**)**

Project: Fundamental Materials Research and Advanced Process Development for Thin-Film CIS-Based Photovoltaics

P.I.: T. J. Anderson

Co-PI's: Sheng S. Li , O. D. Crisalle, and Valentin Craciun

Other Personnel Ryan Acher, Joshua Howard, Chia-Hua Huang, Ryan Kaczynski, Lei Li Kerr, Woo Kyoung Kim, Matt Monroe, Wei Liu, Jiyon Song, Xuege Wang, and Seokhyun Yoon

Subcontract No.: ADJ-2-30630-13

Funding Agency: National Renewal Energy Laboratory (NREL)

Program: Thin-Film Photovoltaics Partnership program

Contact Address: Tim Anderson, P.O. Box 116005, 227 Chemical Engineering Bldg., University of Florida, Gainesville FL 32611-6005, Phone: (352) 392-0882, FAX: (352) 392-9513, E-mail: tim@nersp.nerdc.ufl.edu

1 Progress on Reaction Pathways and Kinetics of $CuInSe_2$ Thin Film Growth from Bi-layer In_2Se_3/CuSe Precursor Films.

Participants: Timothy J. Anderson and Oscar D. Crisalle (Faculty Advisors), Woo Kyoung Kim, Seokhyun Yoon, Ryan Acher, and Ryan Kaczynski (Graduate Research Assistants).

1.1 Objective

In-situ study of the reaction pathways and kinetics of $CuInSe_2$ formation from bi-layer In_2Se_3/CuSe precursor film using time-resolved high temperature X-ray diffraction.

1.2 Accomplishments

1.2.1 Preparation of precursor films

Bi-layer In_2Se_3/CuSe precursor films were grown on sodium-free thin(0.4mm) glass substrates in the PMEE (Plasma-assisted Migration Enhanced Epitaxy) reactor. The crystalline In_2Se_3 bottom layer was grown with a substrate temperature of approximately 400°C. The crystalline CuSe top layer was deposited on the as-grown In_2Se_3 layer at lower substrate temperature condition (~150°C) to minimize any potential reactions between the In_2Se_3 and CuSe layers. The total thickness (~0.6□m) and the atomic composition ([Cu]/[In]~0.94 ; [Se]/[Metal] ~1.2) of the bilayer precursor were measured by SEM and ICP, respectively.

1.2.2 Time-resolved high temperature X-ray diffraction

Time-resolved high temperature X-ray diffraction data were collected using a position sensitive detector(PSD) while the bi-layer In_2Se_3/CuSe precursor films were maintained at a constant temperature in a He(flowrate~100sccm) ambient. The temperature range for the isothermal experiments was between 232 and 275°C. The surface temperature was measured with a type-S thermocouple calibrated against the thermal expansion coefficient of silver. The O_2 content of outlet gas as measured by an O_2 analyzer was less than 0.1 ppm.

Both the consumption of CuSe and In_2Se_3 reactant phases and the formation of $CuInSe_2$ product phase are qualitatively demonstrated in the time dependent spectra shown in Figure 1-1. The phase evolution rates at different temperatures are visually compared in Figure 1-2.

During the phase evolution, no intermediate phases were detected. For quantitative analysis, the mole fractions of reactants (CuSe, In_2Se_3) and product ($CuInSe_2$) were calculated by

measuring the XRD peak area (Figure 1-3).

The atomic composition ([Se]/[Metal]~0.95) as determined by ICP measurement after the isothermal reaction indicated that the excess selenium evaporated during the reaction. Therefore, the following reaction is suggested.

$$2CuSe + In_2Se_3 \rightarrow 2CuInSe_2 + Se\ (evaporated) \quad (1\text{-}1)$$

A preliminary kinetic analysis was performed using the Avrami model, which has been widely used to describe crystalline-to-crystalline phase transformations [1]. According to the Avrami model, the transformation kinetics under isothermal heating is described by

$$\alpha = 1 - exp[-(kt)^n] \quad (1\text{-}2)$$

or

$$ln[-ln(1-\alpha)] = nlnt + n\ lnk \quad (1\text{-}3)$$

where the fractional reaction α represents the volume fraction transformed, k is the kinetic rate constant, and n is the Avrami exponent. The Avrami plots for the isothermal reaction at different temperatures are shown in Figure 1-4.

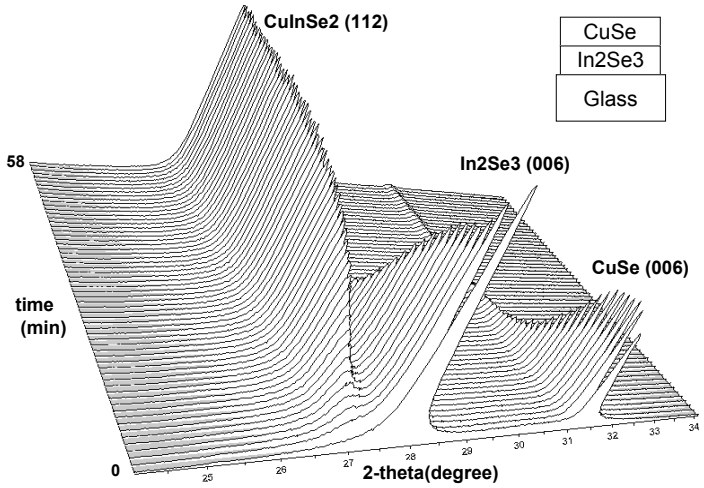

Figure 1-1. Time-resolved *in-situ* X-ray diffraction for isothermal heating at 264°C.

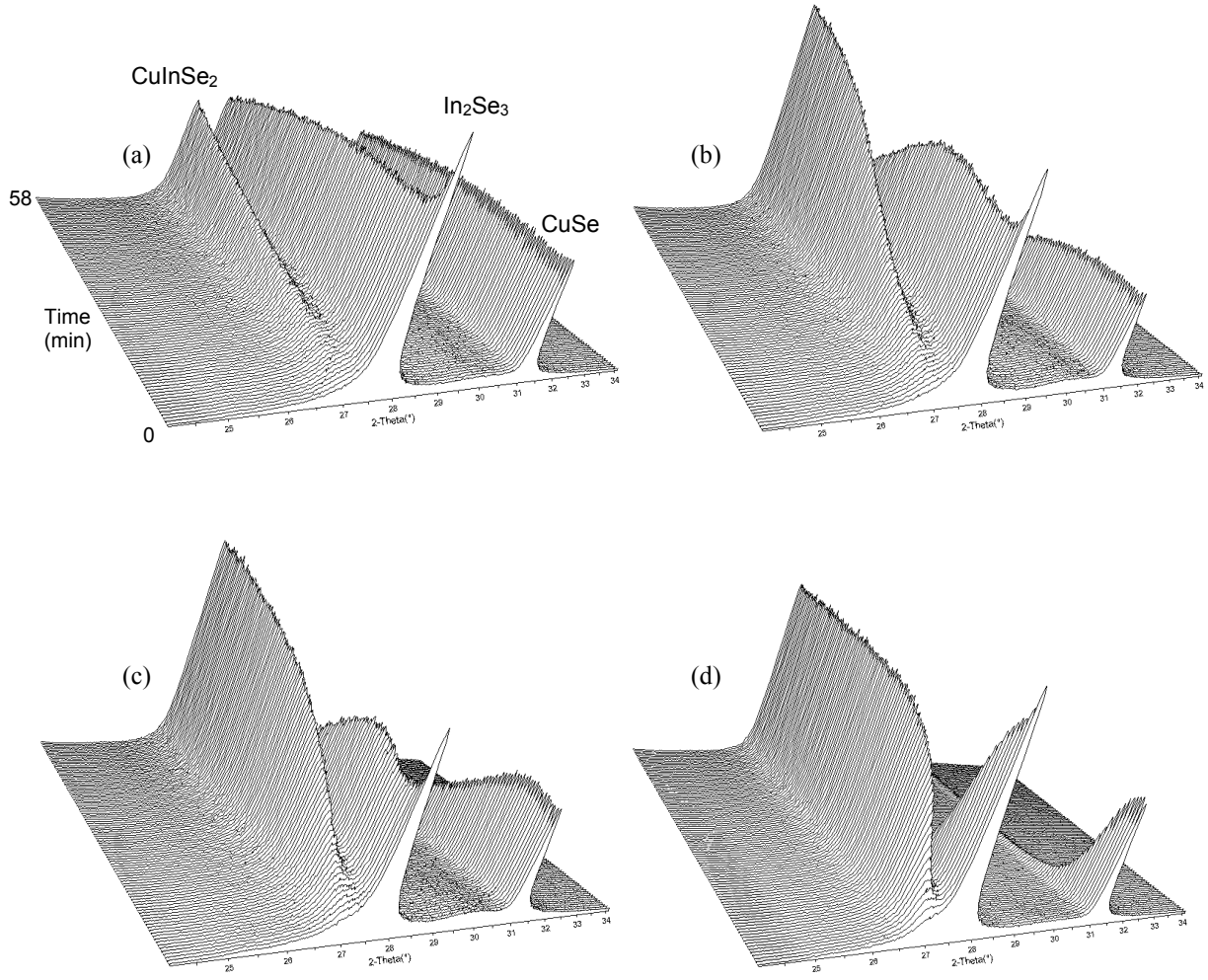

Figure 1-2. Phase evolution during isothermal reaction at different temperatures: (a) 232°C, (b) 243°C, (c) 254°C, (d) 264°C.

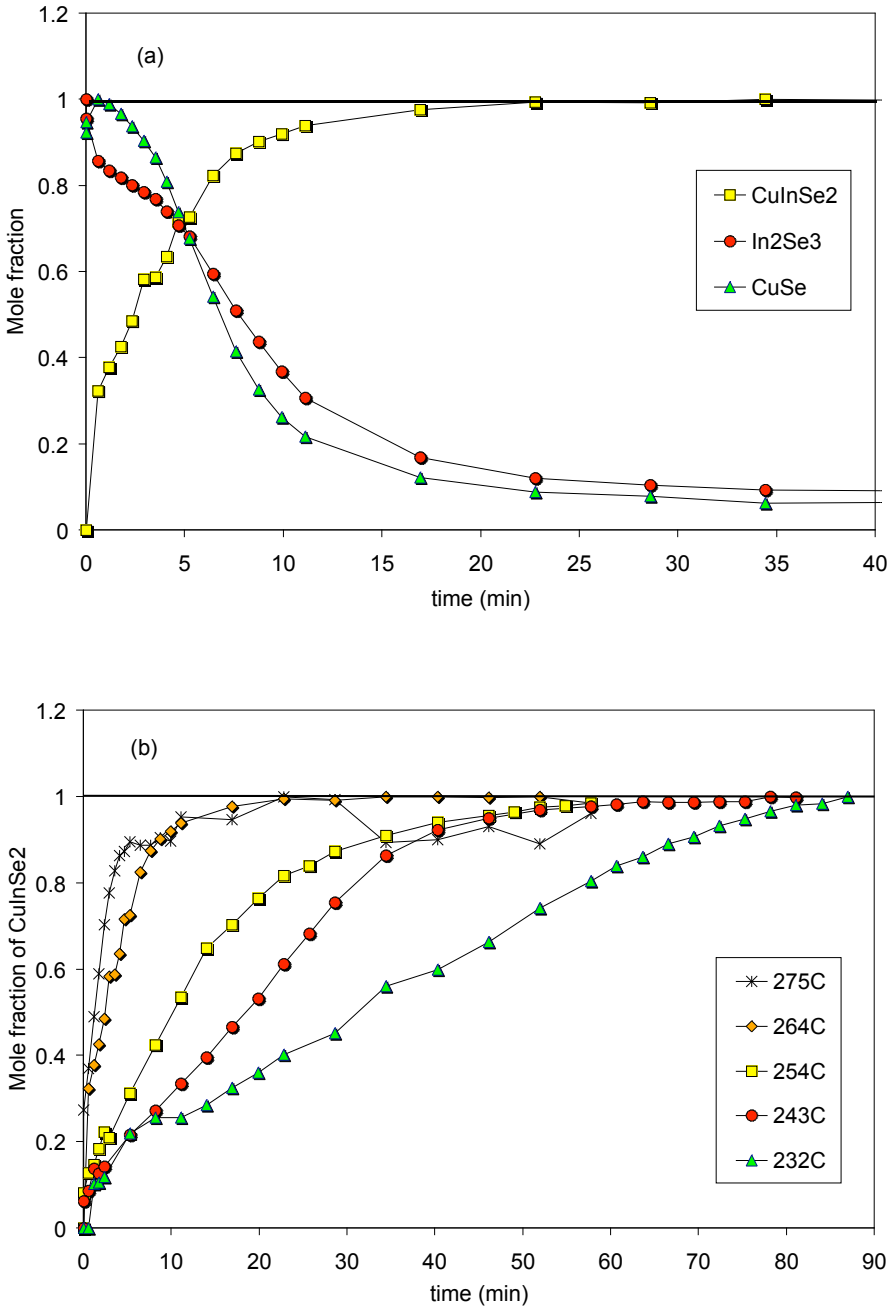

Figure 1-3. (a) Mole fraction changes of reactants (CuSe, In_2Se_3) and product ($CuInSe_2$) for isothermal reaction at 264°C. (b) Mole fraction change of $CuInSe_2$ as a function of time and temperature.

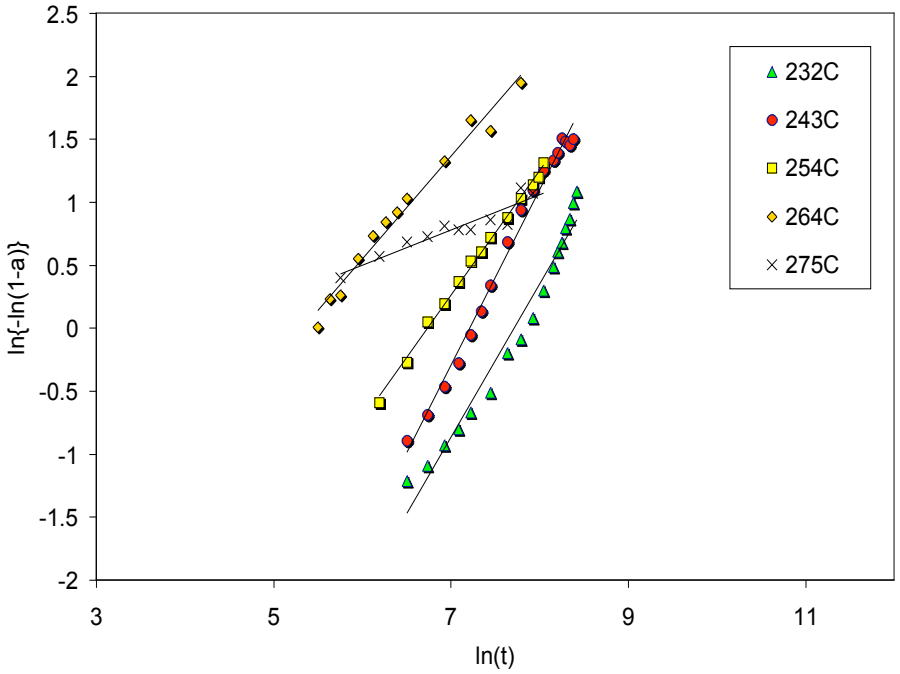

Figure 1-4. Avrami plots for the isothermal reactions at different temperatures.

The Avrami exponents (n) and the kinetic rate constants (k) estimated from Avrami plots are summarized in Table 1-1.

Table 1-1. Estimated rate constants and Avrami exponents for the $CuInSe_2$ formation from In_2Se_3/CuSe bilayer precursor films.

Temperature (°C)	**n**	**k (s^{-1})**
232	1.22	0.000450
243	1.40	0.000741
254	0.99	0.001186
264	0.82	0.004866
275	0.28	0.015128

To estimate the apparent activation energy of this reaction, the logarithm of the estimated rate constant was plotted as a function of reciprocal temperature as shown in Figure 1-5. This Arrhenius plot shows two apparent activation energies in different temperature regions. The estimated activation energies were 97 kJ/mol in the high temperature region (255~275 °C) and 290 kJ/mol in the low temperature region (230~255 °C). These two values of activation energy are much larger than the activation energy (~66kJ/mol) for the $CuInSe_2$ formation from InSe/CuSe bilayer films [2].

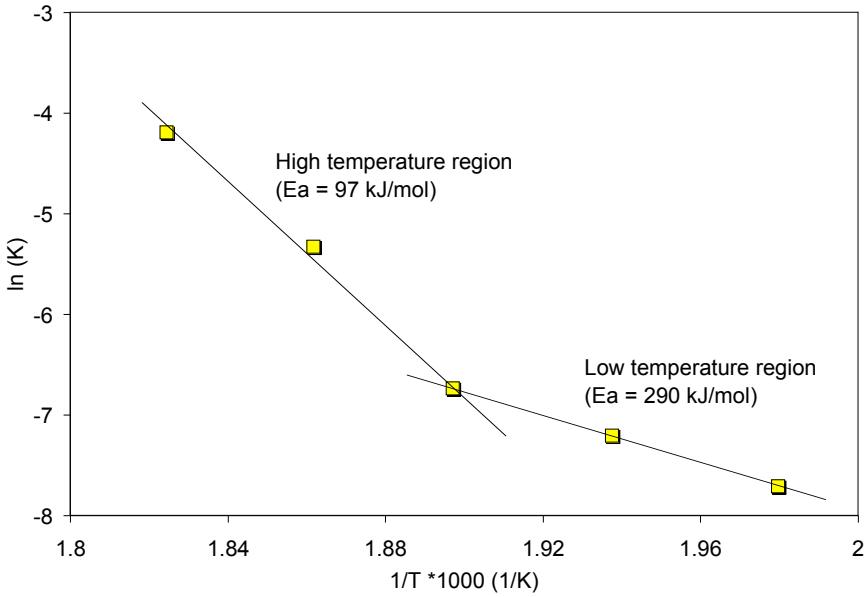

Figure 1-5. Arrhenius plot for the $CuInSe_2$ formation from In_2Se_3/CuSe bilayer precursor films.

1.3 Publications and presentations

[1] S. Kim, W.K. Kim, E.A. Payzant, R.M. Kaczynski, R.D. Acher, S. Yoon, T.J. Anderson, O.D. Crisalle, and S.S. Li, "Reaction Kinetics of $CuInSe_2$ thin films grown from bilayer InSe/CuSe precursors", *J. Vac. Sci. Tech. A (submitted).*

[2] S. Kim, W.K. Kim, E.A. Payzant, R.M. Kaczynski, R.D. Acher, S. Yoon, T.J. Anderson, O.D. Crisalle, and S.S. Li, "Investigation of $CuInSe_2$ Growth Kinetics using Time-resolved High Temperature XRD", *presentation at MRS meeting,* April (2003).

1.4 References cited

[1] F. Hulbert, J. Br. Ceram. Soc.,**6**, 11 (1969)

[2] S. Kim, W.K. Kim, E.A. Payzant, R.M. Kaczynski, R.D. Acher, S. Yoon, T.J. Anderson, O.D. Crisalle, and S.S. Li, "Reaction Kinetics of $CuInSe_2$ thin films grown from bilayer InSe/CuSe precursors", *J. Vac. Sci. Tech. A (submitted).*

2 Deep Level Transient Spectroscopy (DLTS) System Setup and Optimization for $Cu(In_xGa_{1-x})Se_2$ Cell

Participants: Timothy J. Anderson, Oscar D. Crisalle, Sheng S. Li (Faculty Advisors), Woo Kyoung Kim, Lei Li Kerr (Graduate Research Assistants).

2.1 Objective

DLTS system setup and optimization for defect characterization of $Cu(In_xGa_{1-x})Se_2$ solar cell.

2.2 Accomplishments

2.2.1 DLTS system setup

The UF DLTS system consists of a Sula Technologies Deep Level Spectrometer (DLS), a Lake Shore 331S temperature controller, a roughing pump, a liquid nitrogen cryostat, and a circulation pump, as shown in Figure 2-1. The Sula DLS system is composed of two pulse generators, two correlators, and a capacitance meter. The temperature control system, which includes a temperature controller, a liquid nitrogen cryostat, a rough pump, and a variable speed circulation pump, allows precise temperature control for a wide range of temperature from 77 to 400K. The entire system including the temperature control system and Sula DLS system is controlled by a computer using Sula DLTS software, which can be operated in several modes such as capacitance-voltage (C-V) and capacitance-temperature (C-T) as well as DLTS measurement.

2.2.2 DLTS system optimization

To test our DLTS system and find the optimum operation parameters for CIGS cells, CIGS cells provided by Energy Photovoltaics Inc. (EPV) were characterized by C-T, C-V and DLTS measurements.

The results of DLTS measurement performed at a reverse bias(V_R) of 0.4 V, a trap-filling pulse of 0.8V, and a saturation pulse width of 10 ms are shown in Figure 2-2. During the DLTS scan, the temperature ramping rate was limited at 0.1 K/sec or less for the precise temperature control. A small CIGS test cell with area of 1 mm□ 0.8 mm was used to maximize the sensitivity of the DLTS system.

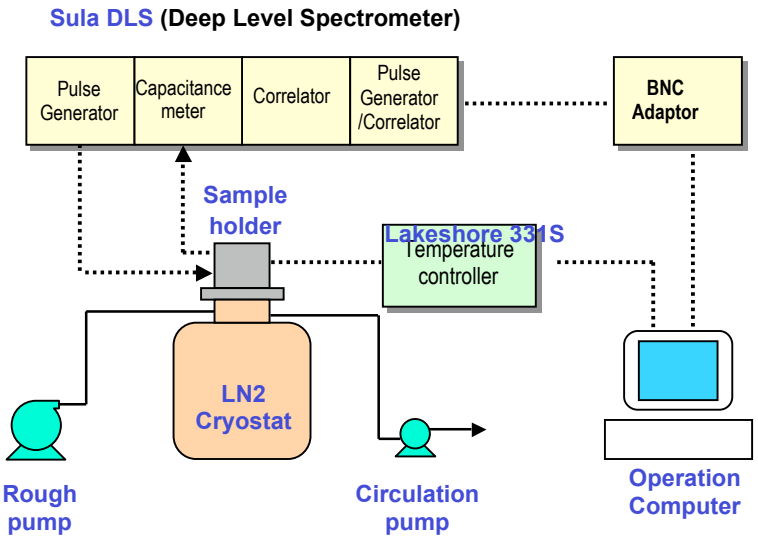

Figure 2-1. Schematic diagram of UF DLTS system.

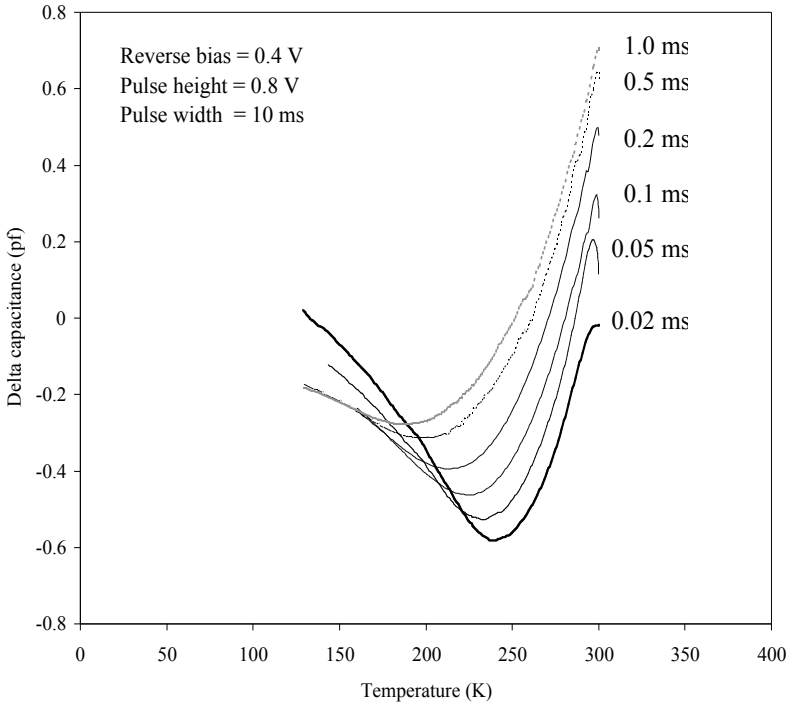

Figure 2-2. DLTS scans for EPV CIGS cell at different rate windows (0.02 ~ 1.0 ms). A hole trap was observed from the scan.

A majority carrier (hole) trap was observed from the DLTS scans shown in Figure 2-2. The activation energy of this hole trap was estimated from an Arrhenius plot, as shown in Figure 2-3. From the Arrhenius plot an activation energy of $E_a = E_v + 0.2$ eV was obtained for this hole trap. The average hole concentration (N_a) obtained from the C-V measurement was about 1×10^{15} cm^{-3} and the trap density (N_T) determined by $N_T \approx (2C/C_0)N_a$ was about 2×10^{13} cm^{-3}.

The results of the DLTS measurement using our DLTS system were in good agreement with the DLTS results determined from the NREL DLTS system performed on the EPV CIGS cell last year by Kerr [1].

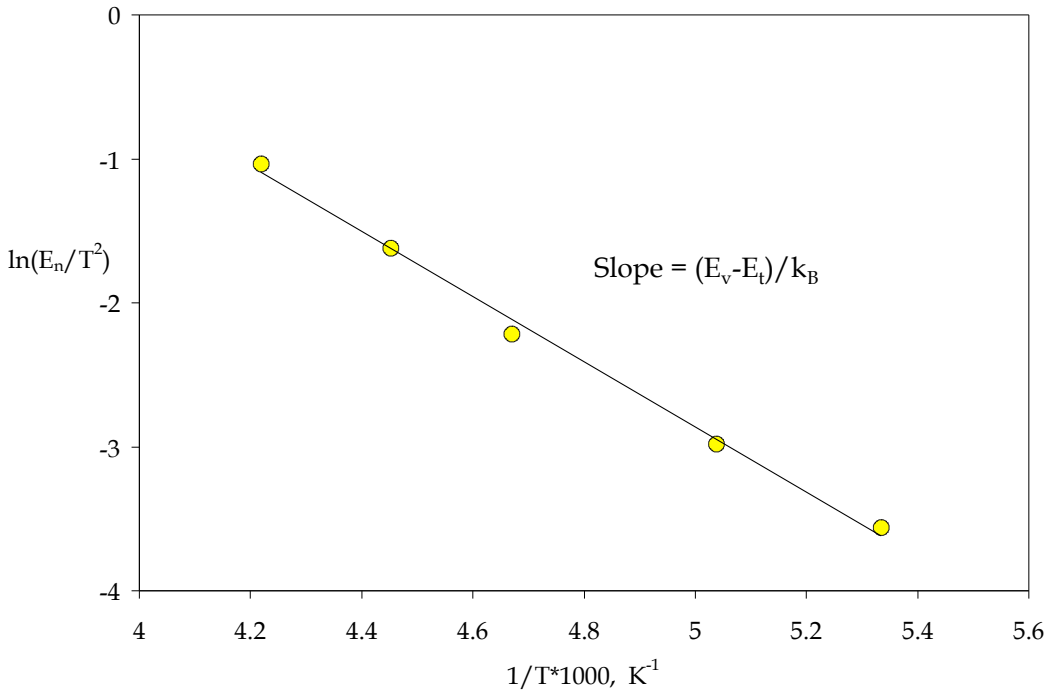

Figure 2-3. Arrhenius plot for the DLTS data shown in Figure 2-2 for the EPV CIGS cell

2.3 References cited

[1] L.L. Kerr, S.S. Li, S. W. Johnston, T.J. Anderson, O.D. Crisalle, and R. N. Noufi, "Deep Level Transient Spectorscopy (DLTS) Characterization of Team CIGS Cells", 20th NCPV Photovoltaics Program Review Proceedings, Golden, CO, (2003).

[2] Sheng S. Li, "Semiconductor Physical Electronics", Plenum Press, New York, 1993.